Sensitivity Evaluation of Mounting Optics Using Elastomer and Bipod Flexures

Paul Mammini[1], Alison Nordt[1], Buck Holmes[2], Dave Stubbs[1]

ABSTRACT

A sensitivity evaluation of mounting 100mm optics using elastomer or bipod flexures was completed to determine the relative effects of geometry, structure, material, thermal and vibration environment as they relate to optical distortion. Detailed analysis was conducted using various finite element-modeling methods. Parts were built and the results were verified by conducting brassboard tests.

What makes this evaluation noteworthy is the two vastly different approaches, and how they both exhibited athermal properties and minimized optical distortion. Materials were carefully selected while the geometry and structure were optimized through analytical iteration.

The elastomeric optical mount consists of 12 equally spaced pads of RTV placed around the circumference of the optic. These pads were sized to maximize stiffness and minimize surface deformations. The surrounding material was appropriately selected in order to contribute to an athermal design.

The bipod flexure optical mount uses three flexures cut from a single piece of material. Each flexure is a bipod oriented to comply radially with changes in temperature. This design is monolithic and uses conventional epoxy at the optical interface. The result is a very stiff athermal design.

This paper covers both opto-mechanical designs, as well as analytical results from computer modeling and brassboard tests.

Keywords: elastomer, bipod flexures, athermal, monolithic

1. INTRODUCTION

The following evaluation was conducted as part of the Space Interferometry Mission (SIM), the first interferometric space scientific mission in a series of NASA Origins Programs. This space observatory uses a triad of interferometric observations of stars to make astrometric measurements at the single digit micro arcsecond level. Such observations are of sufficient quality to infer the existence of earth-size planets orbiting remote stars by detecting the reflex motion of the orbiting motion of these planets on the star. This mapping of likely earth-like planetary systems then forms the basis for compiling a set of targets for future observation missions like Terrestrial Planet Finder (TPF).

In any precision measurement system, one must be diligent in tracking down and minimizing effects of error sources that might corrupt the measurement itself. For SIM, there are many such sources, such as thermal effects, wavefront quality of the optical components, sensor noise, diffraction, etc. It is the purpose of this paper to report on the investigation of thermal effects and wavefront quality of optical components in such a precision system and discuss methods to minimize these errors by athermalizing such optical mounts.

[1]Lockheed Martin Space Systems - Missile Systems Organization - Advanced Technology Center
3251 Hanover Street, Bldg 201, Dept. L9-23, Palo Alto, CA 94304

[2]Jet Propulsion Laboratory- 4800 Oak Grove Drive, Pasadena, California 91109

2. MAM OPTICAL MOUNT

The original intent for the investigation into an athermal optical mount was to improve the thermal stability of the mirror and beamsplitter mount assemblies that were used on SIM's Micro-Arc second Metrology Testbed (MAM). The MAM designs use three, 0.015 in. thick, radial leaf springs (fixed at two ends to an inner gimbal), each with one 304 Stainless Steel tab laser welded at the center of the spring. The tabs attach to the optic 120 degrees apart and are bonded to the optic with epoxy. The bondline thickness was metered using 0.005 in. diameter glass beads. Two variations of this mount were implemented. The two mounts used similar hardware and were otherwise identical with the exception of the epoxy and the assembly method. The first variation used Epibond's 1210-A/9615-10, aka "Blue Death". The second variation used 3M's 2216 epoxy.

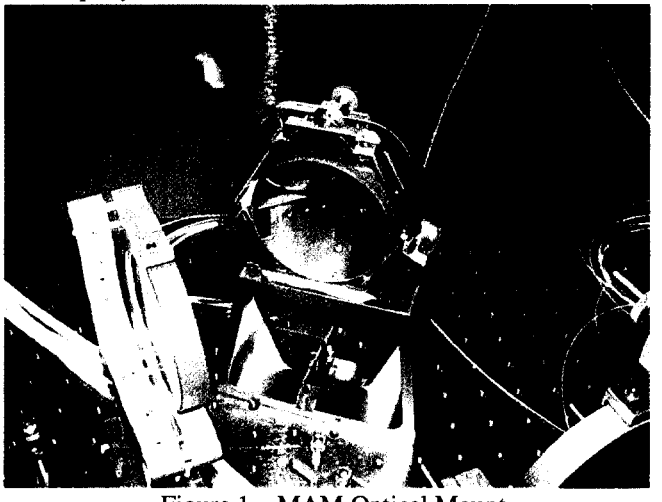

Figure 1. MAM Optical Mount

The thermal stability of each design was tested in a thermally insulated "tent". This test was intended to be a simple test to determine if there were any exceptionally problematic characteristics of the mounts. The test was assembled relatively quickly with equipment and hardware that was readily available. The optical mounts were aligned in front of a Zygo Interferometer, which was also inside of the tent. A thermometer was placed inside the tent next to the optic. A 75-watt light bulb was placed inside the tent, turned on, and left overnight. The light was removed quickly the following morning, attempting not to disturb the tent any more than necessary. The thermometer was read by opening an edge of the thermal blanket a crack and shining a flashlight in. All efforts were made to develop an insulated environment for the test in which thermal gradients across the optic would be minimized as much as possible. The tent environment cooled slowly, taking most of the day to return to room temperature.

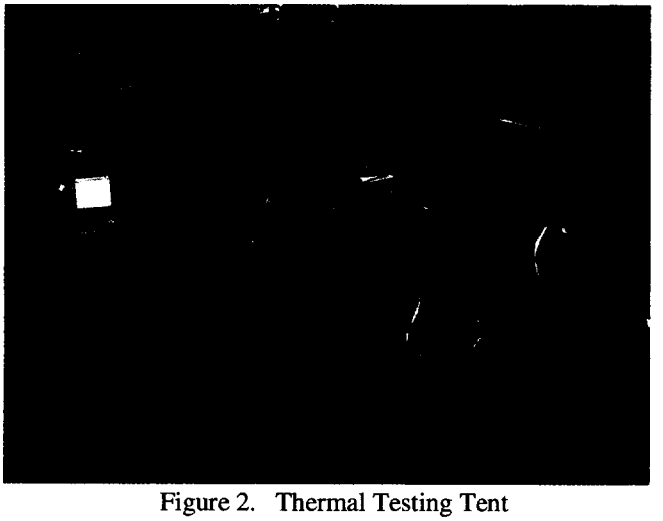

Figure 2. Thermal Testing Tent

Temperature	Time	Wavefront			
(degrees C)	(after start)	*P-V*	*RMS*	*Power*	Comments
-	-	-	-	-	Unmounted Optic, Unaveraged Zygo Data
-	-	0.054	0.009	-0.019	Mounted Optic Prior to Thermal Test
35	-	0.188	0.042	-0.128	
34	-	0.181	0.040	-0.128	
32	-	0.124	0.028	-0.091	
29	-	0.100	0.021	-0.070	
24	-	0.097	0.013	-0.032	Effect of Mounting Tab Stress Visible on Interferogram
23	-	0.099	0.012	-0.026	Effect of Mounting Tab Stress Visible on Interferogram
22	-	0.103	0.009	-0.015	Effect of Mounting Tab Stress Visible on Interferogram
21	-	0.096	0.011	-0.019	Effect of Mounting Tab Stress Visible on Interferogram
-	-	0.080	0.009	-0.005	Room Temp, Flexure Tabs Screws all Loosened

Figure 3. Table shows change in wavefront vs. temperature for the MAM Epibond 1210 mount

Temperature	Time	Wavefront			
(degrees C)	(after start)	*P-V*	*RMS*	*Power*	Comments
		0.080	0.004	0.006	Unmounted Optic
-	-	0.060	0.005	0.001	Mounted Optic Prior to Thermal Test
37	14:15	0.138	0.029	-0.084	
34	14:40	0.100	0.020	-0.062	
33	15:00	0.074	0.012	-0.033	
28	16:30	0.064	0.010	-0.026	
27	17:00	0.066	0.010	-0.023	
25	18:40	0.061	0.010	-0.019	
24	20:30	0.068	0.008	-0.005	
23	21:00	0.063	0.007	-0.007	
23	22:20	0.063	0.007	-0.015	
22	23:00	0.060	0.008	-0.009	

Figure 4. Table shows change in wavefront vs. temperature for the MAM 3M 2216 Mount

In both cases, the first mode frequency of this design was over 300Hz (I-DEAS structural analysis). However, when exposed to a thermal gradient both optics showed a significant deformation.

The MAM Epibond mount developed clear indications of stress at the tab locations during the test. This was not observed on the MAM 3M mount. Loosening the blade flexures slightly improved the wavefront, but did not eliminate the edge lifting at the tab locations. The wavefront distortion of the MAM Epibond mount was plastic; it did not recover from the thermal test. The P-V wavefront value increased 78% (from 1/19 wave to 1/10 wave at 633 nm). This number changed 250% during the test (to 5 waves at the highest temperature).

The MAM 3M mount showed trends in wavefront during the test that were similar to those in the MAM Epibond mount. The MAM 3M mount showed much less hysteresis than the MAM Epibond mount and the optical distortion was elastic. The wavefront after the test was very close to the initial wavefront.

The difference in behavior of these two optical mounts is directly related to both the assembly procedure and epoxy selection. The choice of epoxy is overwhelmingly dominant over the difference in assembling similar parts. Residual stress from assembly can contribute to these differences. We saw in the MAM Epibond mount after the spring (flexure) tabs were loosened, about a 30% change in the wavefront.

3. ATHERMAL MOUNT USING RTV

An alternative mirror mount was designed that utilizes pads of thick RTV adhesive to bond the optic to a metallic cell. The thickness of the RTV pads is designed to allow the mount to be quasi-athermal while the diameter of the pads was designed such that the first mode frequency of the mirror in the mount would be greater than 300Hz.

The mount geometry is shown in Figure 5. The mount cell is made of Kovar and the mirror material is fused silica. Twelve dots of RTV are used to hold the mirror in the cell.

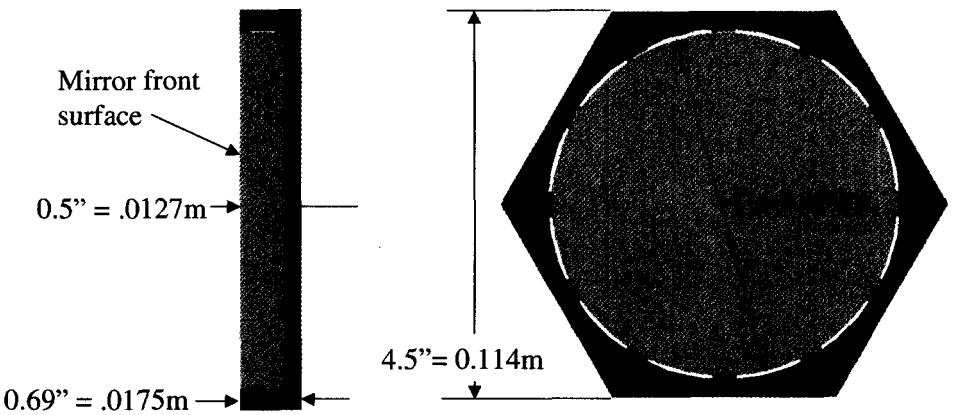

Figure 5. RTV Mount Geometry

The thickness of the RTV dots was determined using the method outlined by John Daly [1] where the thickness of RTV, t_{RTV}, is given by:

$$t_{RTV} = \frac{D_g(\alpha_m - \alpha_g)}{2(\alpha_{RTV} - \alpha_m)} \qquad \text{(Eq. 1)}$$

where D_g = diameter of the optic, α_m = (CTE) Coefficient of thermal expansion of the metal cell, α_g = CTE of the optic and α_{RTV} = CTE of the RTV. The material properties used are given in Figure 6. This formula gives the thickness of the RTV to be 9.16E-4m or 0.036in.

MATERIAL	Modulus (Gpa)	Poisson's Ratio	CTE (ppm/K)	Density (g/cc)
Kovar	138	0.3	5.5	8.36
Fused Silica	72	0.17	0.55	2.2
RTV	0.0035	0.49947	280	1.1

Figure 6. Material Properties for the RTV Mount

If the mount were truly athermal then the diameter of the RTV pads could be made the full thickness of the mirror and the mount would be unaffected by thermal distortions. It is impossible, however, to make the mount perfectly athermal. Therefore distortions of the optic will occur due to temperature changes. In order to minimize these distortions the diameter of the RTV pads should be minimized. Alternatively, the stiffness of the mount depends on the RTV pad diameter and demands a large diameter for the RTV. The diameter of the pads was determined such that it is just large enough to satisfy the stiffness requirement (first mode frequency greater than 300 Hz).

Finite element analysis, using both I-DEAS and Nastran was used to determine the first mode frequency as a function of RTV dot diameter. The mount, mirror and RTV pads were modeled using parabolic

tetrahedron solid elements with at least 4 elements through the thickness of the RTV pads. Several cases were run to determine the sensitivity of the first frequency to RTV dot diameter. The results are shown in Figure 7. The results for the first two modes are shown in Figure 8.

RTV Dot Diameter	1st mode (Piston)	2nd mode (Tip/Tilt)
5.1mm (0.2in)	201 Hz	269 Hz
6mm (0.235in)	252 Hz	317 Hz
6.9mm (0.273in)	294 Hz	371 Hz
7.3mm (0.289in)	315 Hz	398 Hz

Figure 7. Frequency on RTV Dot Diameter

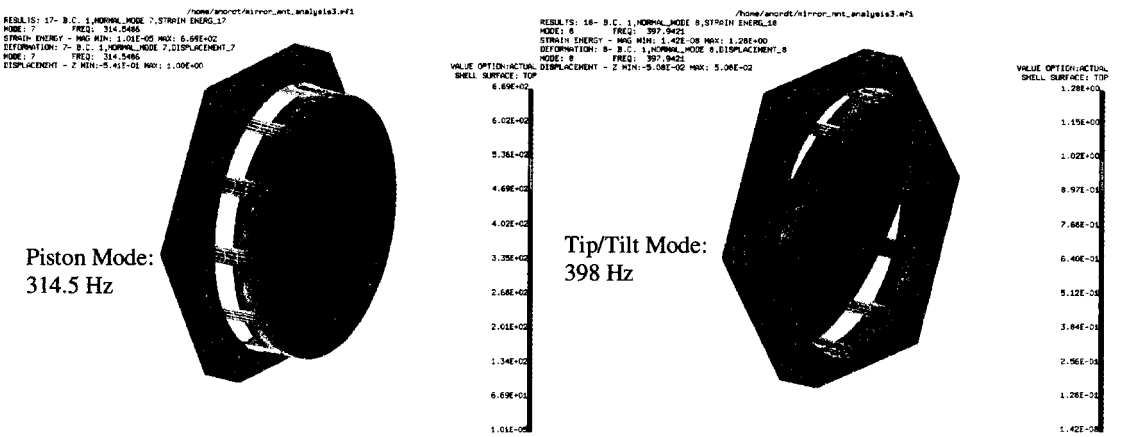

Figure 8. First and Second Modes of the RTV Mount

After the baseline dimensions for the RTV pad thickness and diameter were determined, the mount was analyzed to determine out of plane distortions of the front surface of the mirror due to temperature changes. The finite element model described above was used with a 10°C temperature change imposed on the mount. Displacement, normal to the front surface of the mirror over the entire front surface and the inner 90% of the surface are shown in Figure 9. Over the entire front surface the peak to valley displacement is 1.3nm and over the center 90% of the front surface the peak to valley displacement is 0.8 nm. These surface distortions give P-V wavefront error (assuming wavelength = 500 nm) of $\lambda/191$ for the entire surface and $\lambda/304$ for the center 90% of the front surface.

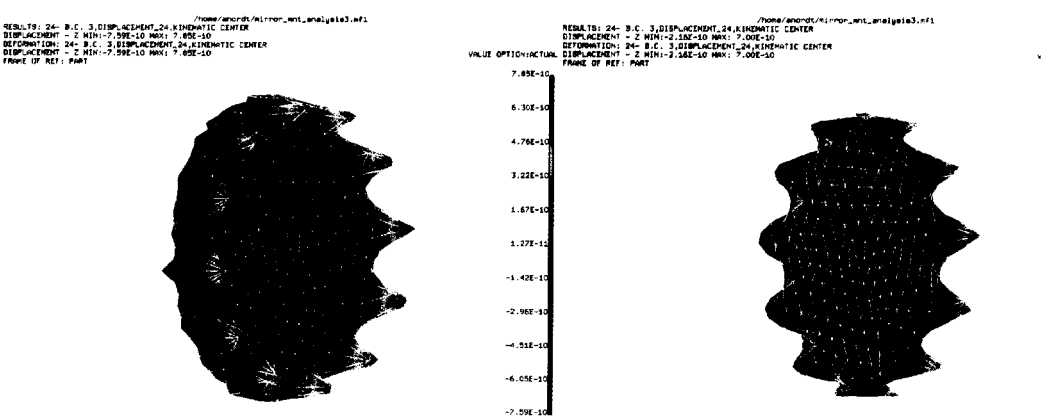

Figure 9. Displacements Normal to the Front Surface of the Mirror Due to a 10°C Temperature Rise. Entire Front Surface (left) and the Center 90% of the Front Surface (right)

The sensitivity to manufacturing and assembly errors and to inaccuracies in the knowledge of the material CTEs was also studied analytically. The same finite element model was used and the material properties were varied. Using Equation 1 an "ideal" RTV thickness was determined for each change in material properties. The thickness of the RTV in the model, however, was not adjusted such that the effect of a less than ideal RTV thickness could be examined. The results of these studies are shown in Figure 10. The results show that the wavefront error does not increase dramatically if the RTV thickness is off by 15%. It is also interesting to note that the wavefront error is less when the RTV is thinner than the "ideal" thickness predicted by Equation 1. It should also be noted that these results are analytical and have not all been verified by test.

CTE RTV (ppm/K)	CTE Kovar (ppm/K)	CTE optic (ppm/K)	Ideal RTV thickness	modeled RTV thickness	P-V WFE full surface	P-V WFE center 90%
280	5.5	0.55	0.916mm	0.993mm	λ/170	λ/272
261	5.5	0.5	0.993mm	0.993mm	λ/191	λ/304
252	6.05	0.495	1.15mm	0.993mm	λ/220	λ/347
308	4.95	0.605	0.728mm	0.993mm	λ/139	λ/223

Figure 10. Sensitivity of the wavefront error to errors in manufacturing or uncertainties in material property knowledge.

4. ATHERMAL MOUNT USING BI-POD FLEXURES

The bi-pod optical mount is a monolithic design that consists of three optical tabs, each supported on a bi-pod flexure. The tabs are attached to the optic with 3M's 2216 epoxy. Like the MAM optical mounts, the bondline thickness is controlled with glass beads. The monolithic Invar part was created using electronic discharge machining (EDM). The EDM uses a charged wire to remove metallic material.

The integral design limits the number of interfaces that can cause unwanted motion, which leads to instability and stress. The bipods flexures are 0.015 in. thick and bend in one axis. The flexures bend to allow the optic diameter to increase in order to accommodate a change (due to temperture) in the diameter of the optic.

Design Space software was used to determine the structural stiffness of the bipod mount and the distortions of the optic caused by thermal gradients. I-DEAS finite element analysis was used to validate the Design Space results. Because of resource constraints, the I-DEAS model was simplified by modeling only the mirror and mirror cell, no bondlines were simulated.

Mode	Shape	Design Space	I-DEAS
1	Piston (focus)	348 Hz	439 Hz
2	Lateral Translation	394 Hz	552 Hz
3	Lateral Translation	395 Hz	552 Hz
4	Tip	446 Hz	622 Hz
5	Tilt	447 Hz	622 Hz
6	Rotation	839 Hz	1120 Hz

Figure 11. Frequency of Bi-Pod Mount

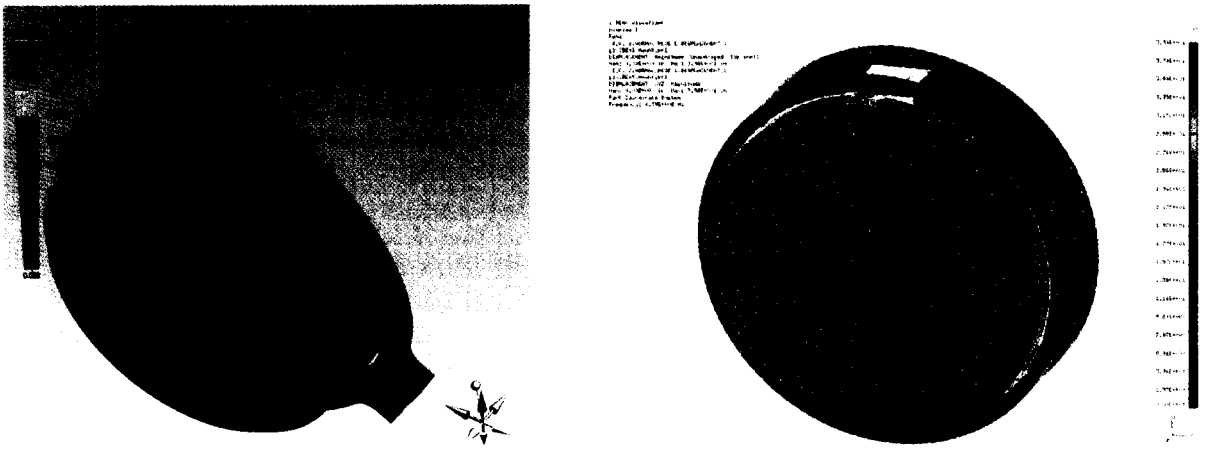

Figure 12. First and second modes of the bi-pod flexure mount

In addition, a series of analysis were carried out including a self-weight deflection analysis of the bipod mount in both a vertical orientation and a tilted 45 degree orientation (not shown). The following is a summary of the Design Space vertical orientation analyses:

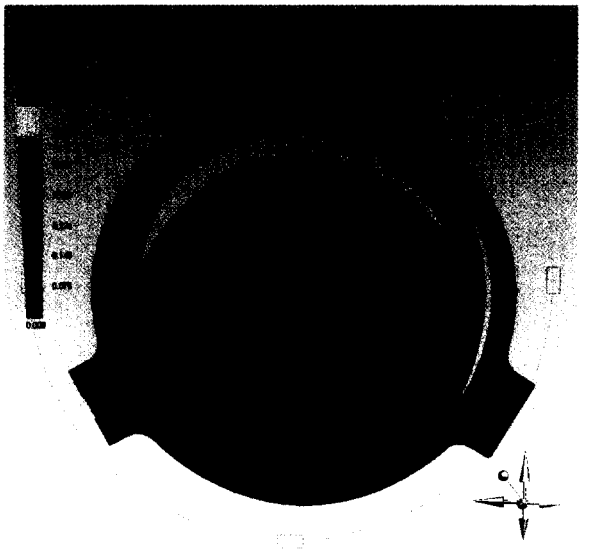

Figure 13. Maximum self-weight deflection of optic relative to cell shown to be 0.0007 inches for the optical axis (horizontal orientation)

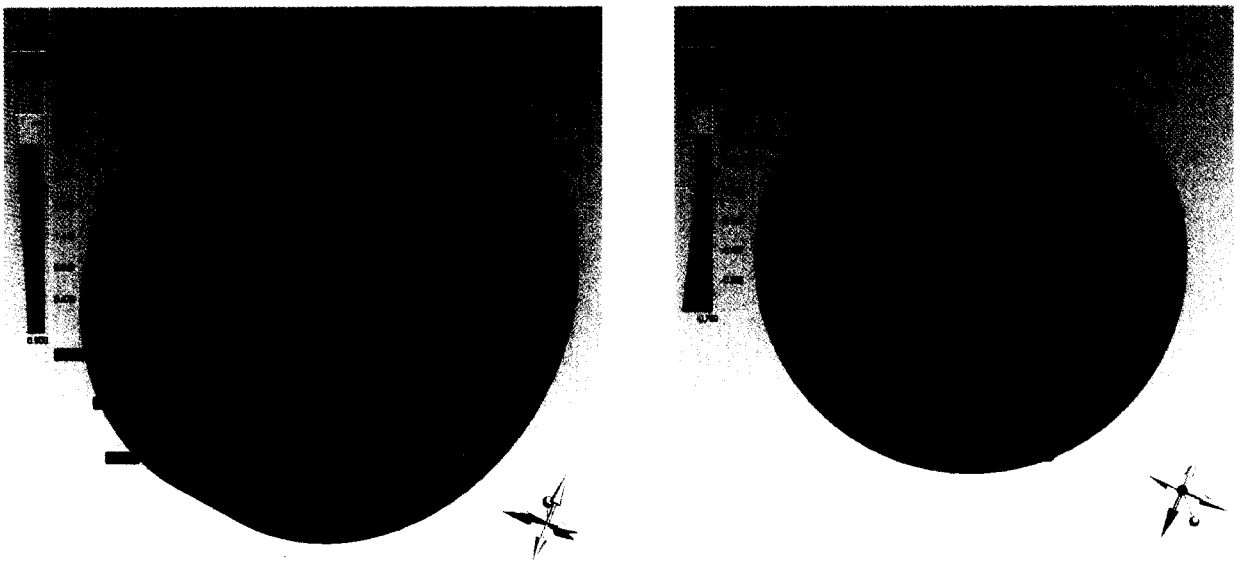

Figure 14. Maximum von mises stress produced in the direction of the optical axis is 4.2 psi (left) and the total deflection of the surface of the optic at bond locations is 0.015 nanometers (right). This is due to self-weight with the optical axis in the horizontal orientation.

Design Space was also used to simulate a 10 degree C change in the environment. The contours are largely parallel, suggesting little distortion of the optic. The model agrees with intuition that a temperature change should produce a minimal effect on the optic, based on bipod geometry and the athermalized nature of the cell. The predicted stress is largely local in nature, due to CTE mismatch at the optic/bond interface.

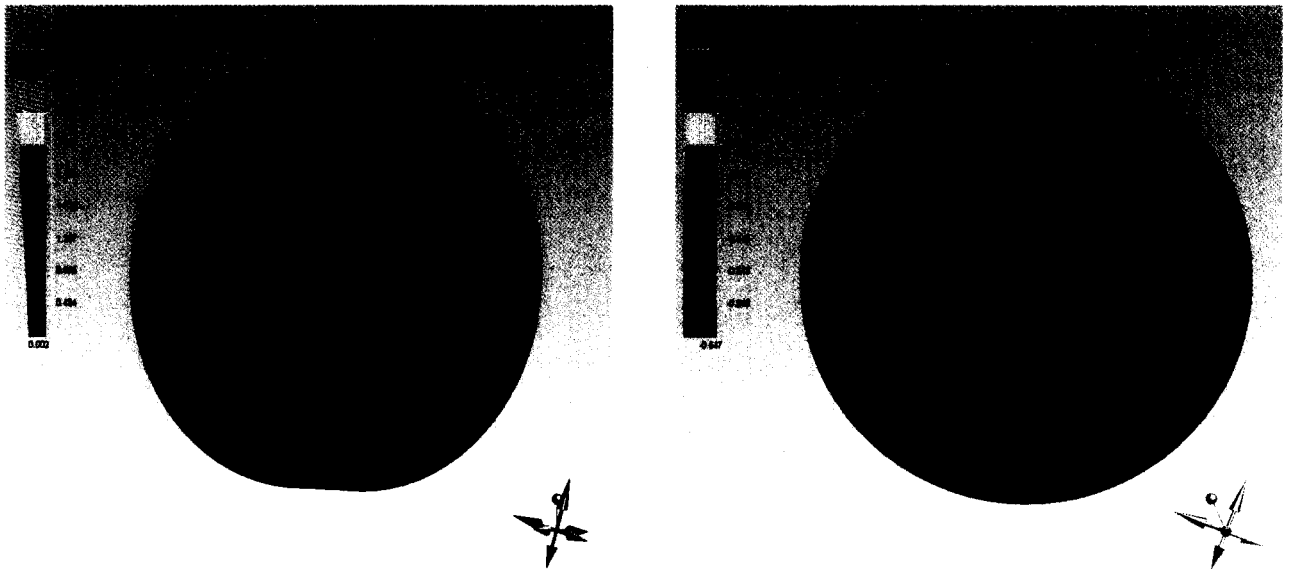

Figure 15. The thermal analyses model predicts that the maximum von mises stress produced in the optic, at bond pad locations, is 3.8 psi. The total deflection of the optical surface in the direction of the optical axis is 28 nanometers.

The geometry of the bi-pod optical mount is inherently stiff and can be configured to be athermal in a number of orientations. In other words, the attachment of the bi-pods can vary depending on the application. Figure 16 shows a bi-pod mount that was designed with the bi-pods turned 90 degrees from the mount that was analyzed in Figures 12 to 15. Through vibration testing, the stiffness-first mode (piston), of the bi-pod mount shown if Figure 16 was measured at 1900 Hz.

Figure 16. Athermal Bi-Pod Optical Mount

In order to compare the thermal stability of the bi-pod mount to the MAM mounts, the bi-pod optical mount in Figure 16 was subjected to the same thermal tests. The bi-pod optical mount showed less variation in wavefront distortion during test (less than 10%, approximately 1/25 of that of variation 1). The maximum Peak-to-Valley (P-V) distortion of the bipod mount was less than either MAM mount and the hysteresis was small as well.

Temperature	Time	Wavefront			
(degrees C)	(after start)	*P-V*	*RMS*	*Power*	Comments
-	-	0.066	0.008	0.022	Unmounted Optic, Unaveraged Zygo Data
		0.060	0.005	0.006	Mounted Optic
-	-	0.076	0.011	0.016	Mounted Optic Prior to Thermal Test
35	14:30	0.083	0.015	-0.039	
32	15:30	0.072	0.013	-0.022	
30	16:30	0.063	0.010	-0.019	
28	17:30	0.064	0.010	-0.008	
26	19:00	0.062	0.007	-0.007	
25	20:30	0.068	0.008	0.001	
24	22:00	0.073	0.009	0.011	
23	24:00	0.072	0.009	0.005	

Figure 17. Table shows change in wavefront vs. temperature for the bi-pod optical mount

5. LESSONS LEARNED

The thermal test for qualifying the optical mounts was not in the original MAM testbed plan. Since schedule and cost were of great concern, the test needed to be carried out quickly and with existing hardware and facilities. In addition and for various reasons, we were not able to conduct the thermal "tent" tests on the exact bi-pod configuration design that we analyzed. The bi-pod design (Figure 16) that was tested in the tent was stiffer (thicker cross section bi-pods) than the bi-pod mount that was analyzed (Figure 12-15). To this end, we predict that the mount shown in Figures 12-15 would contribute less optical distortion than the mount shown in Figure 16.

In an effort to minimize optical distortions caused by thermal gradients, the athermal RTV mounts replaced MAM Epibond like optical mounts on SIM's Diffraction Testbed (DTB). This testbed is operated in a vacuum environment. When cycling in and out of vacuum, DTB is seeing unwanted micro-radian tilts that may be caused by movement of the RTV. The tilts are repeatable and moisture absorption/mass loss of the RTV may be a root cause of this elastic behavior. As predicted through analyses, the mounts exhibit athermal behavior (no optical distortion), but expansion/contraction of the RTV may be causing the micro-radian tilt. At the time this paper was published this phenomenon was still under investigation.

We did not concentrate on obtaining highly accurate values for stiffness and optical distortion due to temperature changes but these tests did allow us to understand how the stability of different opto-mechanical designs compare to one another. As a result, through modeling and analyses it's practical and efficient to design stiff athermal optical mounts and then observe and record the behavior of the built assemblies.

A designer of a successful athermal optical mount design must consider geometry of the mount, properties of the selected bonding agent and the materials used to hold the optic, as well as the handling and use environment. The best designs are possible when the designer includes proper analyses and testing as a part of the athermal sensitivity evaluation.

9. SUMMARY AND ACKNOWLEDGEMENTS

All work described in this publication was carried out at the Jet Propulsion Laboratory and the Lockheed Martin Space Systems Company – Missile Systems Organization - Advance Technology Center by a talented team of dedicated engineers and scientists.

Paul Mammini is a Senior Mechanical Engineer and has been an employee at Lockheed Martin for four years where he has worked on aerospace flight programs and technological testbeds.
Dr. Alison Nordt is a Mechanical Engineer Specialist and has been an employee at LM for four years.
Buck Holmes is a Mechanical Engineer Specialist and has been an employee at JPL for two years.
David Stubbs is a Principal Mechanical Engineer and has been an employee at LM for 23 years.

REFERENCES

[1] "Structural Adhesives for Optical Bonding" course notes by John Daly, SPIE short course taught at Lockheed Martin, 01 June 2001.